



Cite this: *RSC Adv.*, 2023, **13**, 8136

## Recent advances in covalent organic frameworks (COFs) for wound healing and antimicrobial applications

Fatemeh Mohajer, <sup>a</sup> Ghodsi Mohammadi Ziarani, <sup>\*a</sup> Alireza Badiel, <sup>b</sup> Siavash Iravani <sup>c</sup> and Rajender S. Varma <sup>\*d</sup>

Covalent organic frameworks (COFs) are crystal-like organic structures such as cartography buildings prepared from appropriately pre-designed construction block precursors. Moreover, after the expansion of the first COF in 2005, numerous researchers have been developing different materials for versatile applications such as sensing/imaging, cancer theranostics, drug delivery, tissue engineering, wound healing, and antimicrobials. COFs have harmonious pore size, enduring porosity, thermal stability, and low density. In addition, a wide variety of functional groups could be implanted during their construction to provide desired constituents, including antibodies and enzymes. The reticular organic frameworks comprising porous hybrid materials connected via a covalent bond have been studied for improving wound healing and dressing applications due to their long-standing antibacterial properties. Several COF-based systems have been planned for controlled drug delivery with wound healing purposes, targeting drugs to efficiently inhibit the growth of pathogenic microorganisms at the wound spot. In addition, COFs can be deployed for combinational therapy using photodynamic and photothermal antibacterial therapy along with drug delivery for healing chronic wounds and bacterial infections. Herein, the most recent advancements pertaining to the applications of COF-based systems against bacterial infections and for wound healing are considered, concentrating on challenges and future guidelines.

Received 13th November 2022  
 Accepted 4th February 2023

DOI: 10.1039/d2ra07194k  
[rsc.li/rsc-advances](http://rsc.li/rsc-advances)

<sup>a</sup>Department of Organic Chemistry, Faculty of Chemistry, Alzahra University, Tehran, Iran. E-mail: gmohammadi@alzahra.ac.ir

<sup>b</sup>School of Chemistry, College of Science, University of Tehran, Iran

<sup>c</sup>Faculty of Pharmacy and Pharmaceutical Sciences, Isfahan University of Medical Sciences, Isfahan, 81746-73461, Iran

<sup>d</sup>Institute for Nanomaterials, Advanced Technologies and Innovation (CxI), Technical University of Liberec (TUL), Studentská 1402/2, Liberec 1 461 17, Czech Republic. E-mail: varma.rajender@epa.gov



Fatemeh Mohajer was born in Tehran, Iran, and she received her BSc in Applied Chemistry from Bu-Ali Sina University, MSc degree in Organic Chemistry from Azad University in Karaj, and her PhD degree in organic synthesis from Alzahra University, Tehran, Iran under the supervision of Prof. Ghodsi Mohammadi Ziarani, in 2021. She is presently continuing her postdoctoral research

Organic Chemistry with Prof. Mohammadi Ziarani. She published 70 papers and 1 book chapter and has 1 encyclopedia contribution.



Ghodsi Mohammadi Ziarani was born in Iran in 1964. She received her BSc degree in Chemistry from Teacher Training University, Tehran, Iran, in 1987, her MSc degree in Organic Chemistry from the Teacher Training University, Tehran, Iran, under the supervision of Professor Jafar Asgarin and Professor Mohammad Ali Bigdeli in 1991 and her PhD degree in asymmetric synthesis (Biotransformation) from Laval University, Quebec, Canada with Professor Chenevert, in 2000. She is a Full Professor of Organic Chemistry in the chemistry department of Alzahra University. Her research interests include organic synthesis, heterocyclic synthesis, asymmetric synthesis, natural product synthesis, synthetic methodology, and applications of nano-heterogeneous catalysts in multicomponent reactions.



## 1. Introduction

Nanoparticles (NPs) and nanoarchitectures have opened a new world in the domain of materials with diverse properties such as high surface-to-volume percentages along with specific size- and surface availability.<sup>1,2</sup> Applications of NPs largely depend on their unique physical attributes as well as their chemical structures. Molecular building blocks have been linked *via* strong bonds, as exemplified by recently developed constructions namely MOFs,<sup>3–7</sup> ZIFs,<sup>8–15</sup> and (COFs).<sup>8–15</sup> Among them, COFs, as reticular organic framework of porous polymers, have been used in catalytic reactions and biomedical fields such as drug/gene delivery, tissue engineering, and antimicrobials/antivirals.<sup>16–21</sup> Some COFs comprise defined functional groups, such as amines and phenols, applied as Lewis acid-based structures with a porous framework; additionally, COFs with



*Alireza Badiei was born in Iran in 1965. He received his BSc and MSc degrees in Chemistry and Inorganic Chemistry from the Teacher Training University (Kharazmi), Tehran, Iran, in 1988 and 1991, respectively, and his PhD degree in the synthesis and modification of nanoporous materials from Laval University, Quebec, Canada, in 2000. He is currently a full Professor in the Chemistry faculty of Tehran*

*University. His research interests include nanoporous materials synthesis, modification of nanoporous materials, and application of organic-inorganic hybrid materials in various fields such as catalysis, adsorption, separation, and sensors.*



*Siavash Iravani (PharmD, PhD) has worked on several academic research projects at the Isfahan University of Medical Sciences (Faculty of Pharmacy and Pharmaceutical Sciences), including green and eco-friendly synthesis of nanomaterials, plant-derived nanostructures, phytochemical analysis, MXenes and their derivatives, carbon-based nano-composites, drug/gene delivery nanosystems, biomedical engineering, and drug nanoparticles. His previous experience, of more than twelve years, centers on drug development and industrial pharmacy in various capacities including research and development, formulation, and quality control. Dr Iravani has authored over 140 peer-reviewed scientific publications including 19 book chapters and two scientific books.*

tailored pores can provide hydrophobic spatial structures to interact with the bacterial cells.<sup>22,23</sup> These classes of materials have been developed as effectual structures for creating photosensitizers, wherein visible light irradiation can be employed to obtain porphyrin and metalloporphyrin dyes. In this process, molecular oxygen offered singlet oxygen ( $^1\text{O}_2$ ) *via* photocatalytic generation, providing efficient antimicrobial agents for wound healing.<sup>24</sup>

A wide variety of nanomaterials and nanosystems have been constructed in the forms of film, electrospun, nanofiber, membrane, (nano)sponge, and hydrogel, which have been exploited for wound healing/dressing applications;<sup>25</sup> these materials have shown potential against wound bacterial infections.<sup>26</sup> However, COFs with advantages of porosity, specific surface areas, uniform pore sizes, good thermal stability, and ease of functionalization have garnered increasing attention, especially in nano- and biomedicine, namely in wound healing and antibacterial applications, offering suitable platforms for the targeted delivery of antibacterial agents against chronic wounds (Fig. 1).<sup>24</sup> COFs can also be deployed against multidrug-resistant bacteria.<sup>27</sup> The COFs include lightweight elements connected with strong covalent bonds, have low density, high thermal stability, and lasting porosity; they are categorized in two- (2D) or three-dimensional (3D) materials.<sup>28</sup> COF-based structures are metal-free with short-term toxicity owing to their stability under physiological conditions. The degradation of COFs appears difficult under normal conditions but needs more evaluations and studies.<sup>29</sup> They are typically fabricated using a controllable condensation reaction. Such architectures have low density and thermal stability with tunable pore sizes and structures, thus rendering COFs as exceptional porous materials.<sup>30</sup>

COFs are leading-edge materials encompassing covalent bonds with large surfaces and pores, which have proven their prowess in various applications namely, drug delivery, therapy,



*Prof. Rajender Varma (H-Index 126, Highly Cited Researcher, 2016, 18, 19, 20, 21, 22) born in India (PhD, Delhi University 1976) is a senior scientist at U.S. EPA with a visiting position at Technical University of Liberec, Czech Republic. He has over 48 years of multidisciplinary research experience ranging from eco-friendly synthetic methods using microwaves, ultrasound, etc. to greener assembly of nanomaterials and sustainable appliances of magnetically retrievable nanocatalysts in benign media. He is a member of the editorial advisory board of several international journals, published over 930 papers, and awarded 17 U.S. Patents, 9 books, 28 book chapters, and 3 encyclopedia contributions with 63800 citations.*



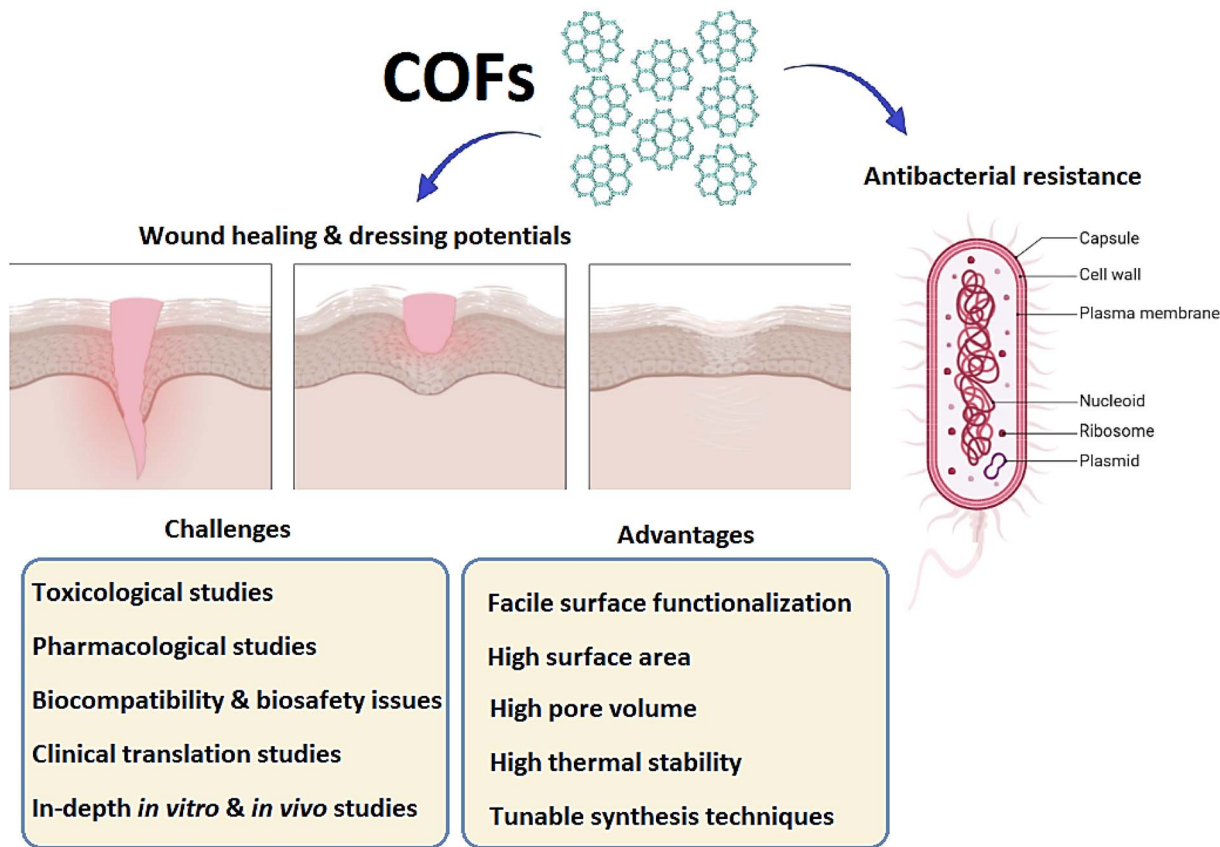


Fig. 1 COFs with wound healing/dressing and antibacterial effects: advantages and challenges.

diagnostics, biotechnology, and heterogeneous catalysis.<sup>15,31–36</sup> In this context, their wound-healing applications as therapeutic agents are deliberated in this review. The wound repair procedure is a highly complex biological procedure, which transpires during human injury; several biological pathways have been developed to respond to human injury.<sup>37</sup> The skin shields the body from several vulnerabilities and assaults.<sup>38</sup> When the wound is inflicted, bacteria attack and bond at the wound spots to create infections disrupting the wound healing process.<sup>39,40</sup> Thus, wound coverings are of immense importance in controlling wound infection and healing the skin.<sup>41–43</sup> Typically, antibiotics have combined into the wound to stop infections,<sup>44,45</sup> although, the overuse of antibiotics may cause poison and bacterial resistance.<sup>46,47</sup>

According to the increasing antibiotic resistance, designing and applying a suitable biofilm on the wound surface might be helpful to control infections in the healing process. Treatment through reactive oxygen species (ROS),<sup>38</sup> such as  $H_2O_2$ , is a practicable tactic to resolve antibiotic resistance, however, one of the challenges is low therapeutic efficiency. Thus, an ionic COF nanozyme with antibacterial properties has been applied *via* glucose-triggered activities in contrast to traditional antibacterial agents; herein, glucose is converted to hydrogen peroxide to decrease the toxicity of hydroxyl radicals. On the other hand, the adhesion of ionic COF nanozyme with the bacterial membrane could improve the healing properties.<sup>48</sup> In

view of the generation of bacteria during infections, wound healing is an important aspect to be considered in terms of health issues.<sup>49</sup> Conventional antibiotics have been routinely applied to combat pathogenic bacteria, but they may develop bacterial resistance.<sup>50</sup> Bacteria create the biofilm through bacterial communities inactivating antibiotics,<sup>51</sup> thus, novel antibacterial agents/systems are in immense demand to address this problem as exemplified by nanomaterials,<sup>52</sup> hydrogels,<sup>53</sup> and peptides<sup>54</sup> to efficiently kill pathogenic bacteria, with targeting properties.<sup>55,56</sup>

COFs have been deployed in many areas such as adsorption and catalysis due to their unique physicochemical properties.<sup>57–60</sup> Yaghi *et al.* synthesized COF-1 and COF-5 in 2005, and four linkage kinds of COFs were created comprising boroxines and boronic esters, imines, triazine, and ketoamines COFs.<sup>61–63</sup> A series of imide-linked COFs were synthesized by Yan's group *via* the imidization reaction in 2014.<sup>64</sup> The prepared PI-COFs displayed thermal stability and specific surface area. In addition, several methods have been reported to synthesize COFs, such as solvothermal, ionothermal, microwave synthesis, and template surface synthesis.<sup>65</sup> All these methods need high operating temperatures for reactions and may release volatile organic compounds (VOC). Hence, it is necessary to develop a green and facile method for synthesizing COF materials. Ionic liquids (ILs), have emerged as greener alternative solvents to conventional solvents in a diverse range



of chemical manipulations and has garnered considerable attention from researchers.<sup>65</sup> In 2018, Fang and co-workers prepared some 3D ILs containing COFs through IL as a green solvent.<sup>66</sup>

*N*-Nitrosamines as a class of compounds with potent carcinogenicity and may have widespread occurrence throughout the environment.<sup>67</sup> Thus, the isolation, removal, and detection of these hazardous compounds should be considered seriously. COF-based materials can be applied to remove *N*-nitrosamines from the environment, which has been of the utmost importance.<sup>68,69</sup> In one study, clover-shaped nano-titania functionalized COFs were deployed for the dispersive solid phase extraction of *N*-nitrosamines from drinking water.<sup>70</sup> Besides, there is an environmental issue related to COFs. They may produce nitrosamines, nitramines, and amides through

a photo-oxidized process, leading to possible carcinogenicity, mutagenicity, and reproductive effects.<sup>71</sup> Other agents for nitrosation are unprotonated amines, which are present in COFs; there is much attention on the nitrosation of secondary amines to provide stable secondary *N*-nitrosamines as a toxic compound.<sup>72</sup> Different techniques have been introduced for synthesizing COFs, such as mechanochemical grinding, solvothermal, microfluidic, ionothermal, microwave-assisted, and interfacial polymerization synthesis techniques.<sup>73</sup> In some of the reported synthesis processes, dimethylformamide (DMF) was utilized.<sup>74</sup> Since the usage of the solvent DMF alongside other reagents was ascertained as the main source of nitrosamine impurities, this should be considered in future explorations to avoid possible toxicity.<sup>67</sup>

In continuation of our ongoing research on medicinal chemistry and drugs,<sup>75,76</sup> herein, we aim to recapitulate the quantitative and qualitative studies on nanoporous material-based COFs in wound healing studies with antibacterial attributes.

## 2. Quantitative studies on the reticular organic framework-recent activities

According to the keyword search in Scopus, we uncovered 3914 papers in document types, comprising 84.6% research articles and 12% review papers, with a limited number of chapter book chapters (~0.5%), which revealed the innovation in this subject area with a lack of compiled book chapters or books related to COFs (Fig. 2) (Scopus).

Based on documents by subject areas, the chemistry of COFs attained the first rank with 28.4%, followed by material science

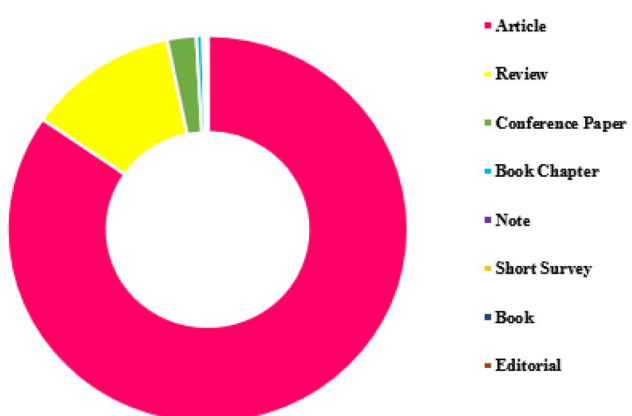


Fig. 2 Document types among 3914 documents from 1991 to 2022 (Scopus).

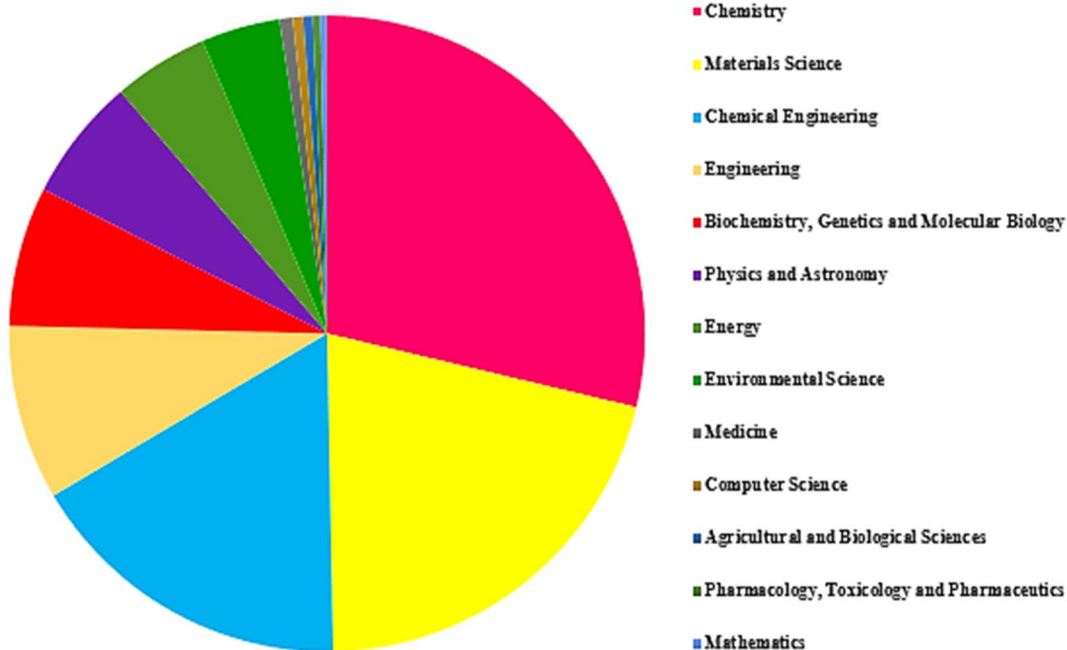
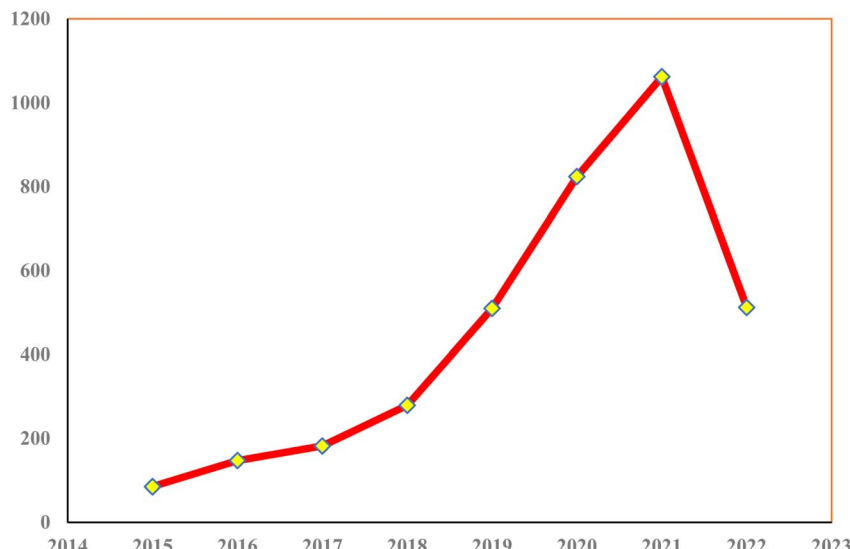


Fig. 3 Documents by subject area among 3914 documents from 1991 to 2022 (Scopus).





**Fig. 4** Publication trends in the “COF” research area between 2015 to the end of 2021 (Scopus)

~20.7%, chemical engineering (16.6%), biochemistry, and astronomy (Fig. 3) (Scopus).

The general analysis illustrated that the publication trend in the “COF-based” research began before 2015; however, the interest among researchers towards COFs is tapering off (Fig. 4) (Scopus).

To analyze the most applied words in the articles and the list of keywords related to COFs, the keyword field was extracted from the RIS data file, as depicted in Fig. 5. There are 6 clusters related to COFs, cluster one with 135 items, anodes, cathodes, biomedical applications, electrochemical performance, and lithium batteries, followed by cluster two, 79 items, absorption, physical chemistry, and luminescence, The third cluster has 78 items such as gas adsorption, mass transfer, and zeolite, while the fourth cluster has 67 items namely carbon dioxide and catalyst and CO<sub>2</sub> reduction, fuel cells, and the fifth cluster with

64 items, such as dyes, and adsorbents; the sixth cluster has 17 members. Consequently, the medical applications of COFs as a newer component were considered for this review; closely associated keywords are visualized with the same color, and a relevant distance based on the map was pictured (Scopus).

### 3. COF-based systems with wound healing and antimicrobial applications

### 3.1. COFs united nanofiber for wound covering

Zhang and co-workers introduced COF as a wound healing structure in 2022 owing to their persuasive structures as drug carriers in biomedicine. The unique belongings of COFs were deployed in wound therapeutics, and they could be applied as targeted drug carriers.<sup>77</sup> Yellow solid, TAPB-DMTA-COF, was produced by the treatment of 2,5-dimethoxyterephthalaldehyde (DMTA) with 5'-(4-aminophenyl)-[1,1':3',1"-terphenyl]-4,4'-diamine (TAPB) in acetonitrile and acetic acid. Then, DMTA and curcumin<sup>78</sup> were mixed to obtain CUR@COF, which in addition to TAPB-DMTA-COF, followed by incorporation with polycaprolactone nanofibrous films generated CUR@COF/PCL NFM<sup>s</sup> *via* the electrospinning process. The CUR@COF/PCL nanofibrous membranes (NFM<sup>s</sup>) for pH-triggered drug release prepared by the electrospinning process were applied to release CUR by protonation under acidic conditions to heal wounds and skin rebirth.<sup>77</sup> CUR was released as an antioxidant and PCL was a synthetic biopolymer employed in biomedical applications in terms of biodegradability and biocompatibility (Fig. 6). The antioxidant and antimicrobial activities and cytotoxicity of biocompatible NFM<sup>s</sup> were examined. *In vivo* wound healing of CUR@COF/PCL NFM<sup>s</sup> was examined in an animal by wound contraction, histopathological evaluation, and immunofluorescence staining (Fig. 7); its low cytotoxicity and good biocompatibility were ascertained.<sup>77</sup> The antibacterial and antioxidant properties were tested with the sustained release of

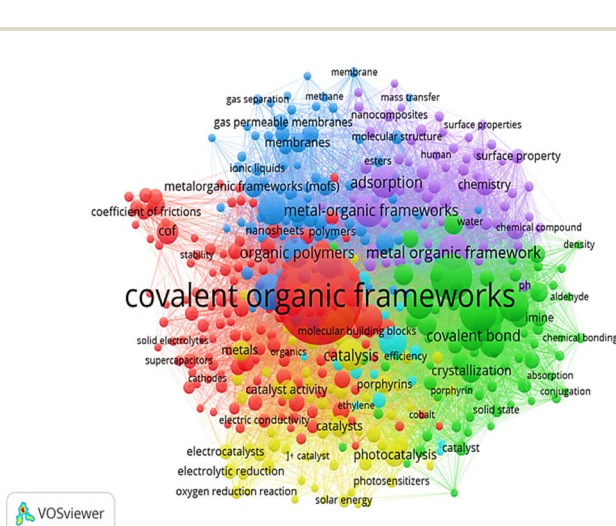


Fig. 5 Network visualization for keyword search results on COFs (Scopus).

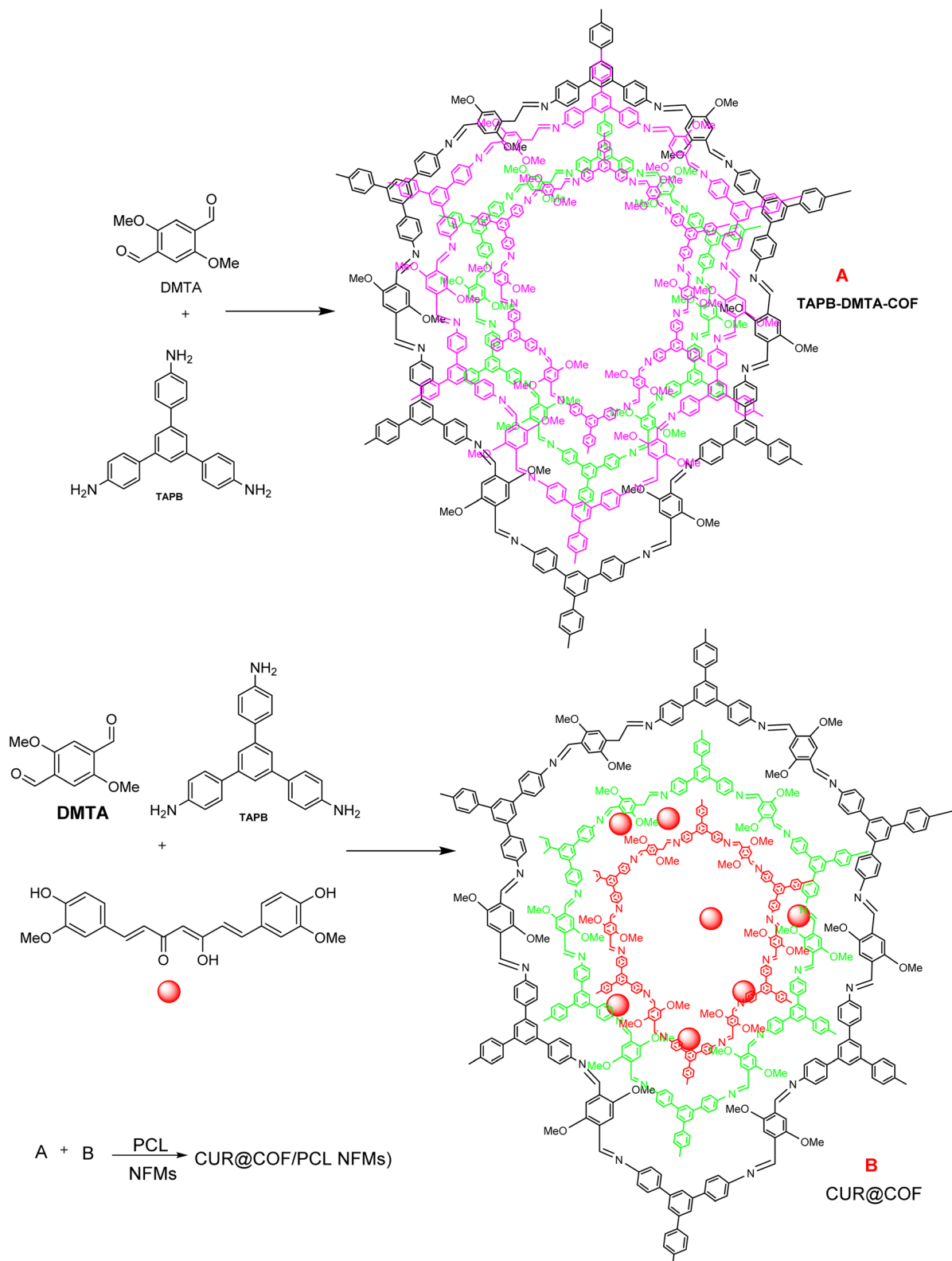


Fig. 6 The generation of antimicrobial CUR@COF/PCL NFM. Redrawn with permission from ref. 77.

CUR by Fickian diffusion. CUR@COF/PCL NFM have good biocompatibility, reduced the inflammatory factors, and encouraged angiogenesis for wound healing procedures.<sup>79,80</sup>

### 3.2. Porphyrin-COFs for wound healing

Collaborative antibacterial and anti-inflammatory attributes of a porphyrin-COF structure have been introduced as

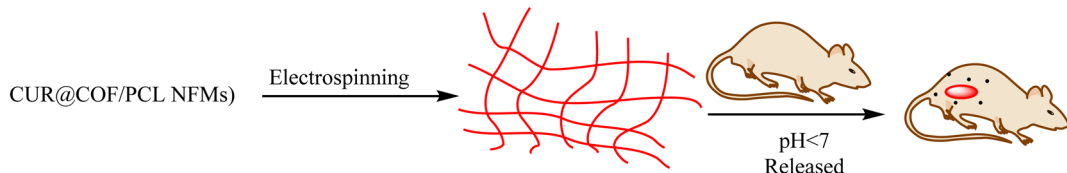


Fig. 7 Drug-release process by CUR@COF/PCL NFM. Reproduced with permission from ref. 77.

a curative option in skin wounds.<sup>81</sup> The polymerization of 5,10,15,20-tetrakis(4-aminophenyl)porphyrin (Tph) with 2,5-dihydroxyterephthaldehyde<sup>42</sup> provided purple-black DhaTph-membrane as a porous host structure COF in the  $\text{H}_2\text{O}/\text{CH}_2\text{Cl}_2$  media using HOAc. The COF was reacted with a 1-hexane solution of ibuprofen (IBU) to generate IBU@DhaTph-membrane for managing IBU as a classic anti-inflammatory drug. A large-area porphyrin-COF membrane was captured with ibuprofen (IBU) to provide IBU@DhaTph-membrane by a singlet oxygen ( $^1\text{O}_2$ ) group and manageable IBU release (Fig. 8). The mice presented a systematic epidermal layer, and the epidermal thickness was close to the normal skin. Also, IBU@DhaTph-membrane has anti-inflammatory and anti-bacterial action, non-toxic interfaces, air permeability, and photothermal result, therefore, the new granulation tissues and the development of novel epidermis through the wound healing procedure ensue.<sup>81</sup>

### 3.3. MOF@COF-based nanozymes

A hybrid MOF@COF nanozyme was synthesized to enhance the performance efficiency of MOFs as dynamic centers with the metallic structure along with the applied COFs as the hierarchical nano-cavities to grow the binding pockets to offer enhanced bacterial inhibition by the tailored pore

Microenvironment.<sup>22</sup> Hierarchy-tailored MOF@COF nanozyme with activated position sites was designed for therapeutic applications *via* non-covalent interactions to trap the bacteria by hairy structure and the spiky COF for killing bacteria *via* the generation of the ROS.<sup>38</sup>

NM-88 was designed through the solvothermal process<sup>82</sup> by the treatment with  $\text{FeCl}_3 \cdot 6\text{H}_2\text{O}$  and 2-aminoterephthalic acid (2-NH<sub>2</sub>-BDC) in DMF. The nanoscale NM-88 was provided by 1,3,5-triformylphloroglucinol (Tp) and 1,2-dichlorobenzene (*o*-DCB)/EtOH into the Pyrex tube and sonicated with acetic acid. After cooling, the dark brown powder ensued as NM-88(CHO), which was mixed with 1,3,5-triformylphloroglucinol (Tp), and 4,4',4''-(1,3,5-triazine-2,4,6-triyl)trianiline<sup>78</sup> in *o*-DCB/ethanol in a Pyrex tube. After sonication and then the addition of acetic acid followed by heating, the reaction mixture afforded a yellowish-brown precipitate as  $\text{NMC}_{\text{Tp-TTA}}$ . It has been envisioned that this nature-inspired approach could accelerate the proposal of different enzyme imitators for treating various bacterial diseases (Fig. 9).<sup>22</sup> It was found that  $\text{COF}_{\text{Tp-TTA}}$  enhanced the catalytic and therapeutic activity of NM-88 nanozyme with an antibacterial effect and negligible toxicity. According to the experimental studies, the catalytic activity depended on pH, the temperature of nanozymes, and substrate concentrations.<sup>22</sup>

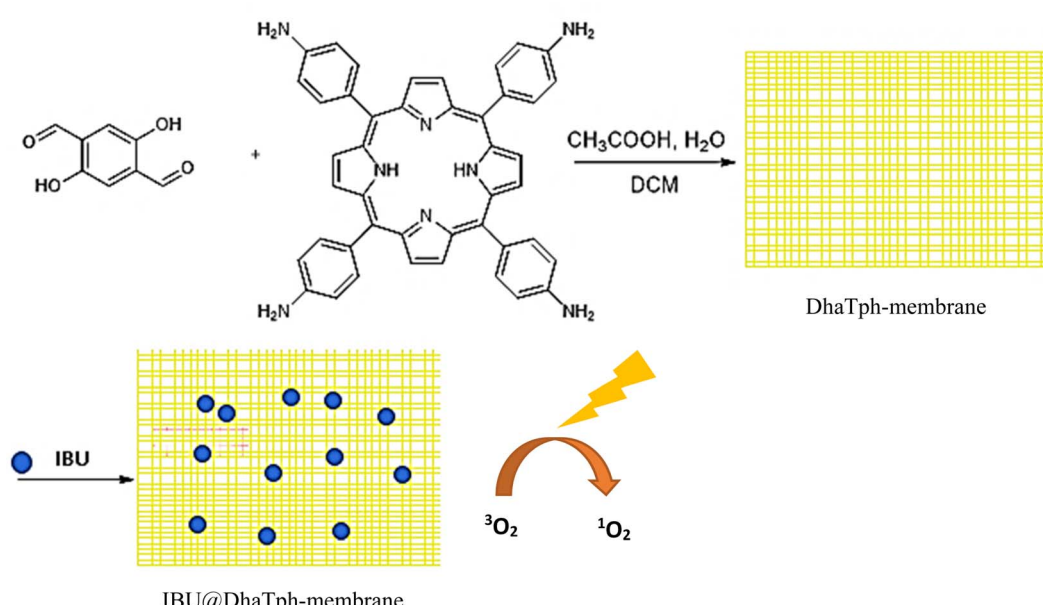


Fig. 8 The preparation of multifunctional antimicrobial IBU@DhaTph-membrane. Reproduced with permission from ref. 81.



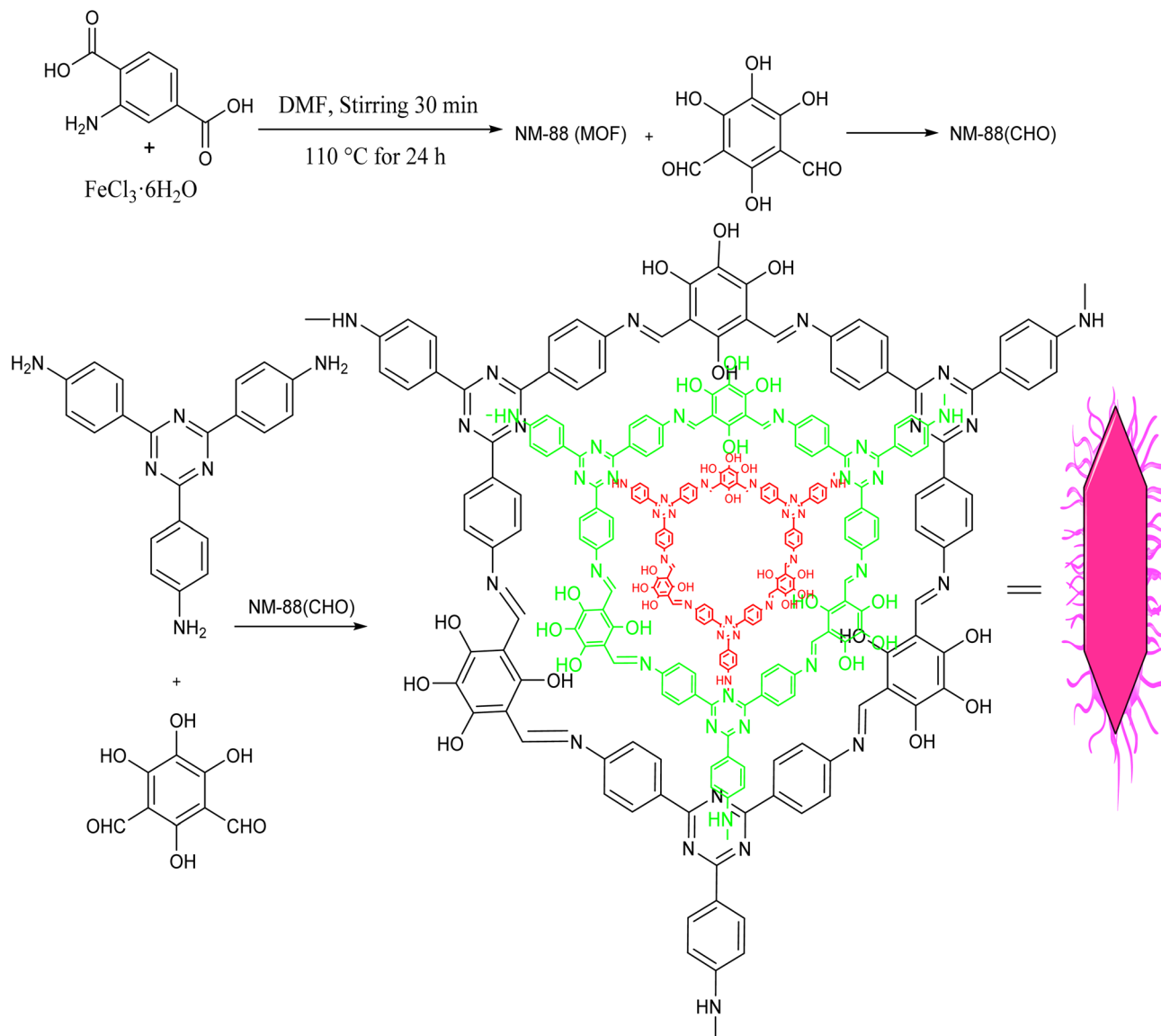


Fig. 9 The preparation of  $\text{NMC}_{\text{TP-TTA}}$  hybrid nanozyme. Reproduced with permission from ref. 22.

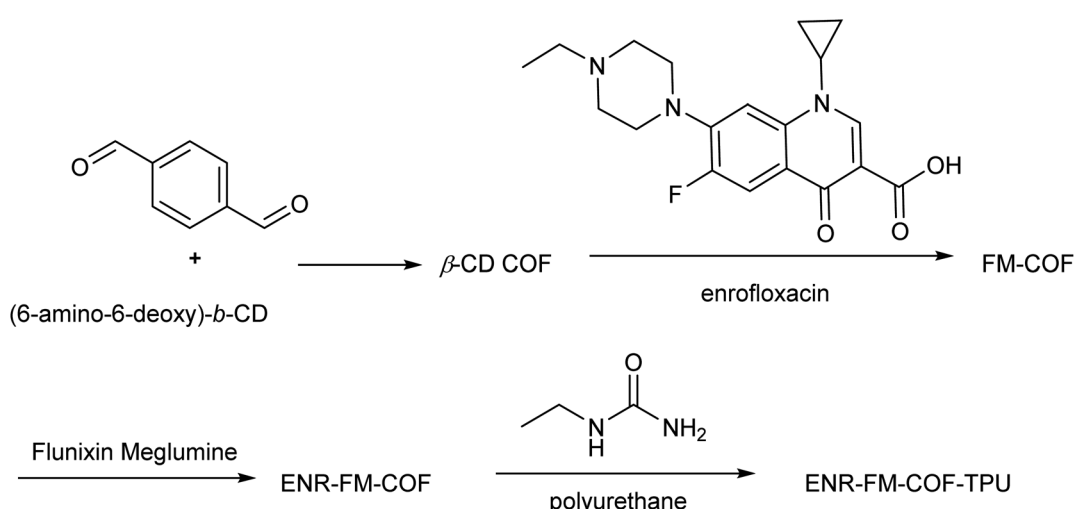


Fig. 10 The preparation of ENR-FM-COF-TPU. Reproduced with permission from ref. 87.

### 3.4. COFs as photosensitizers for antibacterial photocatalytic therapy

Antibacterial photocatalytic treatment can be deployed by COFs with suitable therapeutic efficiency. In 2021, COF-based structure was introduced by Sun *et al.*, which was employed as an antibacterial agent for photocatalytic therapy.<sup>83</sup> The acridine-based COF was produced through the treatment of 2,4,6-triformylphloroglucinol (TFP) with 3,6-diaminoacridine (DAA) as the Schiff base skeleton to afford trifomyl phloroglucinol diamino acridine (TPDA) for harvesting light with narrow optical bandgap from the UV to the near-infrared area,<sup>84</sup> it displayed antibacterial actions for Gram-negative and positive microorganisms where TPDA functioned as a new light-sensitive material for photodynamic treatment.<sup>83</sup> Proflavine-like 3,6-diaminoacridine (DAA) generates ROS in the presence of visible

light,<sup>85</sup> which upon reaction with 2,4,6-triformylphloroglucinol (TFP) could deliver antibacterial photocatalytic therapy (APCT) with photocatalytic potential.<sup>86</sup> According to cytotoxicity data, TPDA has low toxicity and good biocompatibility. TPDA is used as a therapeutic agent with high ROS generation capability. TPDA produced by light to yield electron-hole pairs, therefore, the free radicals created and dispersed in TPDA, which inactivated the bacteria with photocatalytic activity.<sup>86</sup>

### 3.5. The electrospun fibrous film containing a cyclodextrin COF with antibacterial effects

Cyclodextrin ( $\beta$ -CD)-based COFs endowed with antibacterial activity were designed through the electrospun fibrous membrane approach and deployed for wound healing.<sup>87</sup> Skin wounds are frequently infected by pathogenic bacteria

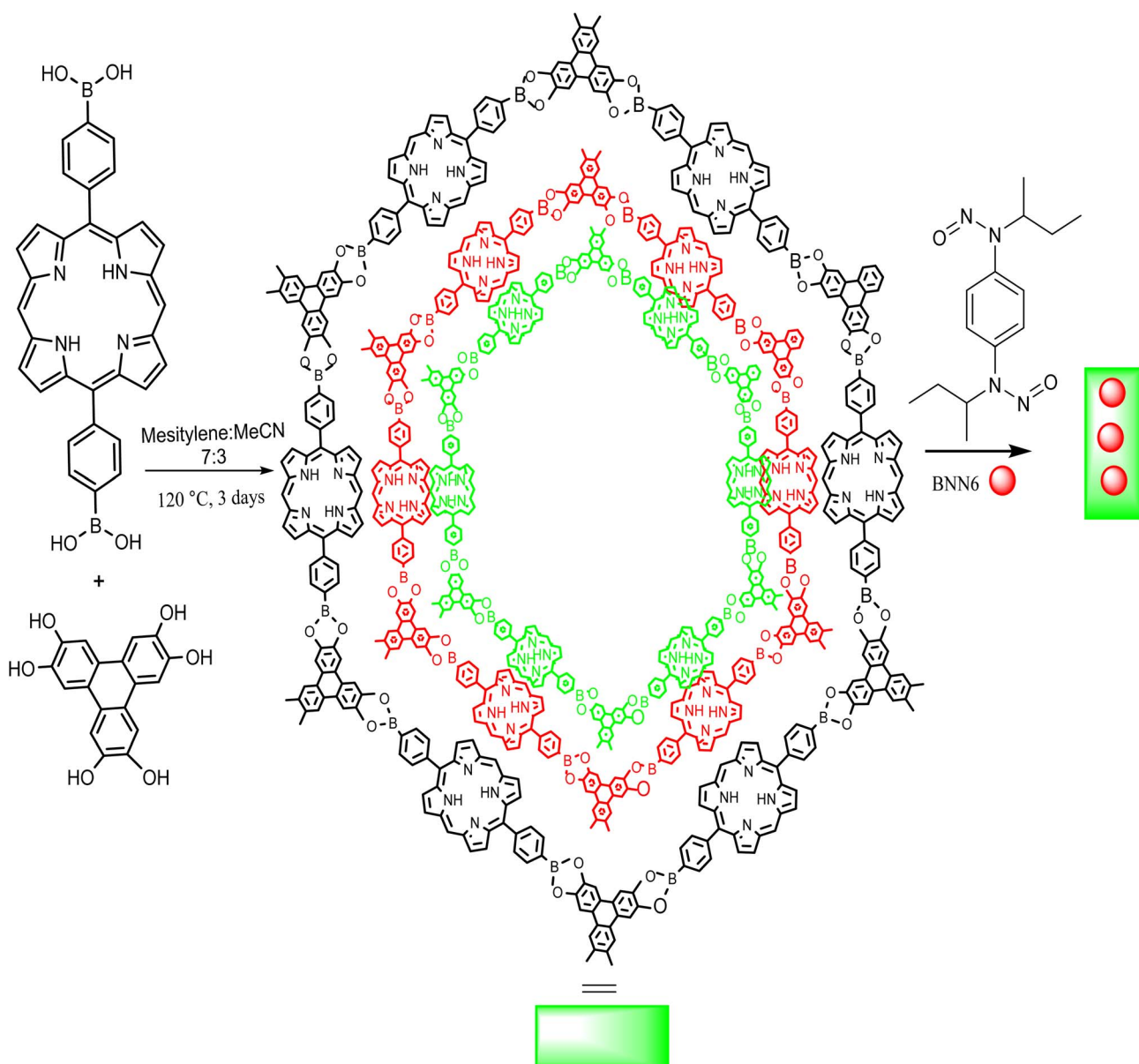


Fig. 11 The preparation of TP-Por-CON. Reproduced with permission from ref. 83.



obstructing the wound healing process, identifying a great challenge in clinical treatment. Thus, wound dressings are of great assistance to inhibit bacterial infections during the wound healing process.<sup>87</sup>  $\beta$ -CD COF<sup>88</sup> as a light yellow solid was generated by the treatment of heptakis (6-amino-6-deoxy)- $\beta$ -CD (Am7CD) with terephthalaldehyde (TPA) in EtOH/H<sub>2</sub>O/CH<sub>3</sub>-COOH. The  $\beta$ -CD COF (ENR-COF) was acquired by mixing the drug and COF in MeOH, along with the addition of enrofloxacin (a fluoroquinolone antibiotic). Besides, the flunixin meglumine was laden on  $\beta$ -CD COF to prepare FM-COF. An electrospinning solution was secured by thermoplastic polyurethane (TPU), DMF, and ENR-COF or FM-COF, which could fabricate the fiber. The electrospun fibers were designed by  $\beta$ -CD COF, ENR-COF, FM-COF, and ENR-FM-COF to generate COF-TPU, ENR-COF-TPU, FM-COF-TPU, and ENR-FM-COF-TPU, respectively. However, ENR-FM-COF-TPU has been shown to be more advantageous among others; it was fabricated by the reaction of enrofloxacin, flunixin meglumine, and polyurethane, with  $\beta$ -CD COF through the electrospinning process and is endowed with hydrophobic behavior and high water with antibacterial activities for wound therapeutics (Fig. 10).<sup>87</sup>

### 3.6. Light-activated COFs for photodynamic and photothermal antibacterial therapy

Typically, COFs are carbon-based constituents encompassing light atoms (carbon, nitrogen, oxygen, and borane) with

biomedical activities.<sup>83</sup> Porphyrin-created COF (TP-Por-CON) was synthesized for photothermal/photodynamic antibacterial therapy under red light radiation. Besides, *N,N'*-di-sec-butyl-*N,N'*-dinitroso-1,4-phenylenediamine (BNN6) was captured into the crystalline pore to trigger the release of NO under red-light irradiation. Accordingly, TP-Por-CON@BNN6 was designed for killing Gram-negative and positive bacteria, which could be applied as a wound-healing agent.<sup>83</sup> To synthesize TP-Por-CON@BNN6, the porphyrin-built COF was synthesized *via* the esterification of 5,15-bis(4-boronophenyl)-porphyrin with 2,3,6,7,10,11-triphenylenehexol (HHTP). Then, the boronic ester COF was created through the reaction of HHTP corners with the porphyrin units, and the spare monomer separated through washing. TP-Por-CON was encapsulated in *N,N'*-di-sec-butyl-*N,N'*-dinitroso-1,4-phenylenediamine (BNN6) for gaseous therapy<sup>89</sup> deploying a NO donor (Fig. 11). The TP-Por-CON@BNN6 was endowed with photothermal, photodynamic, and gaseous therapy that could be exploited in a comprehensive treatment (Fig. 12).<sup>83</sup>

### 3.7. Ionic COF as an active cascade catalyst

GOX-on-Fe-iCOF (GFeF) was prepared; initially, iCOF was synthesized by the reaction of 1-methyl-2-pyrrolidinone (NMP), in 5,10,15,20-tetra(4-pyridyl)-21*H*,23*H*-porphine (TPyP) and *p*-xylylene dibromide using polyvinylpyrrolidone (Mw 30 000). The synthesized iCOF was chelated with ferrous chloride at room temperature to create porphyrin-based iCOF (Fe-iCOF), which

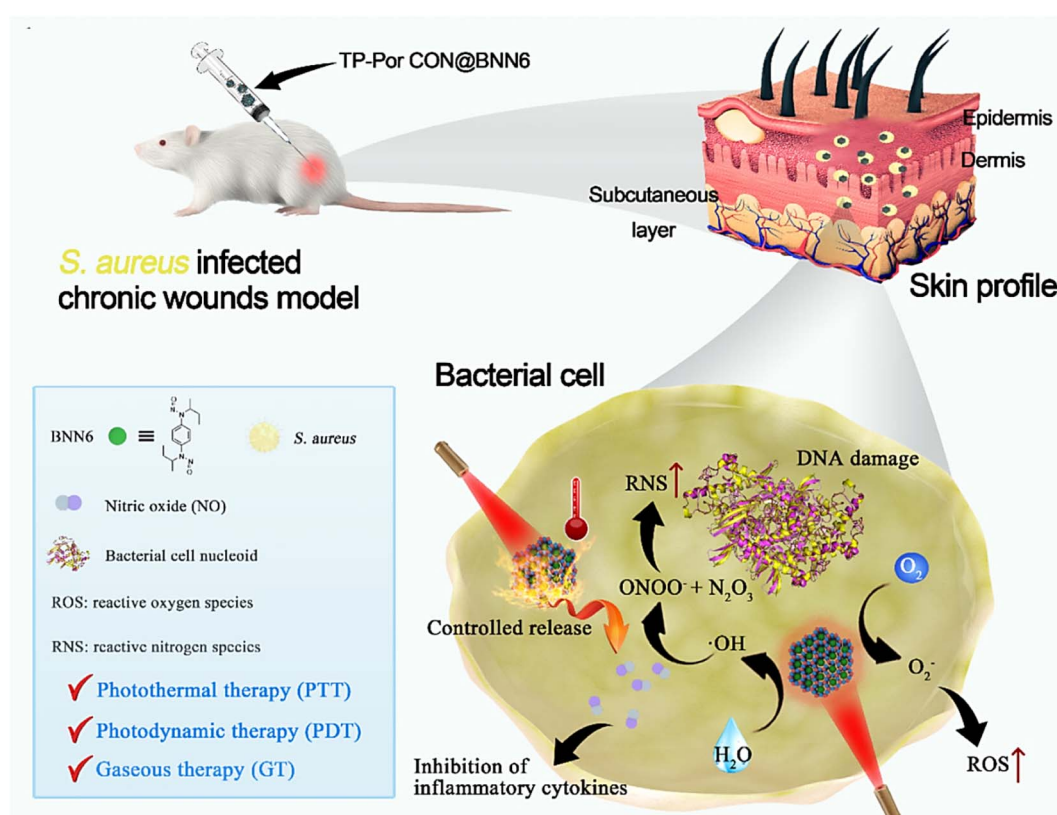


Fig. 12 The TP-Por-CON@BNN6-integrated heterojunction exhibited synergistic photothermal/photodynamic and gaseous therapeutic effects (the related mechanisms), destroying the bacterial cells through ROS formation, temperature elevation, and NO release. Reproduced with permission from ref. 83 Copyright 2021 American Chemical Society.



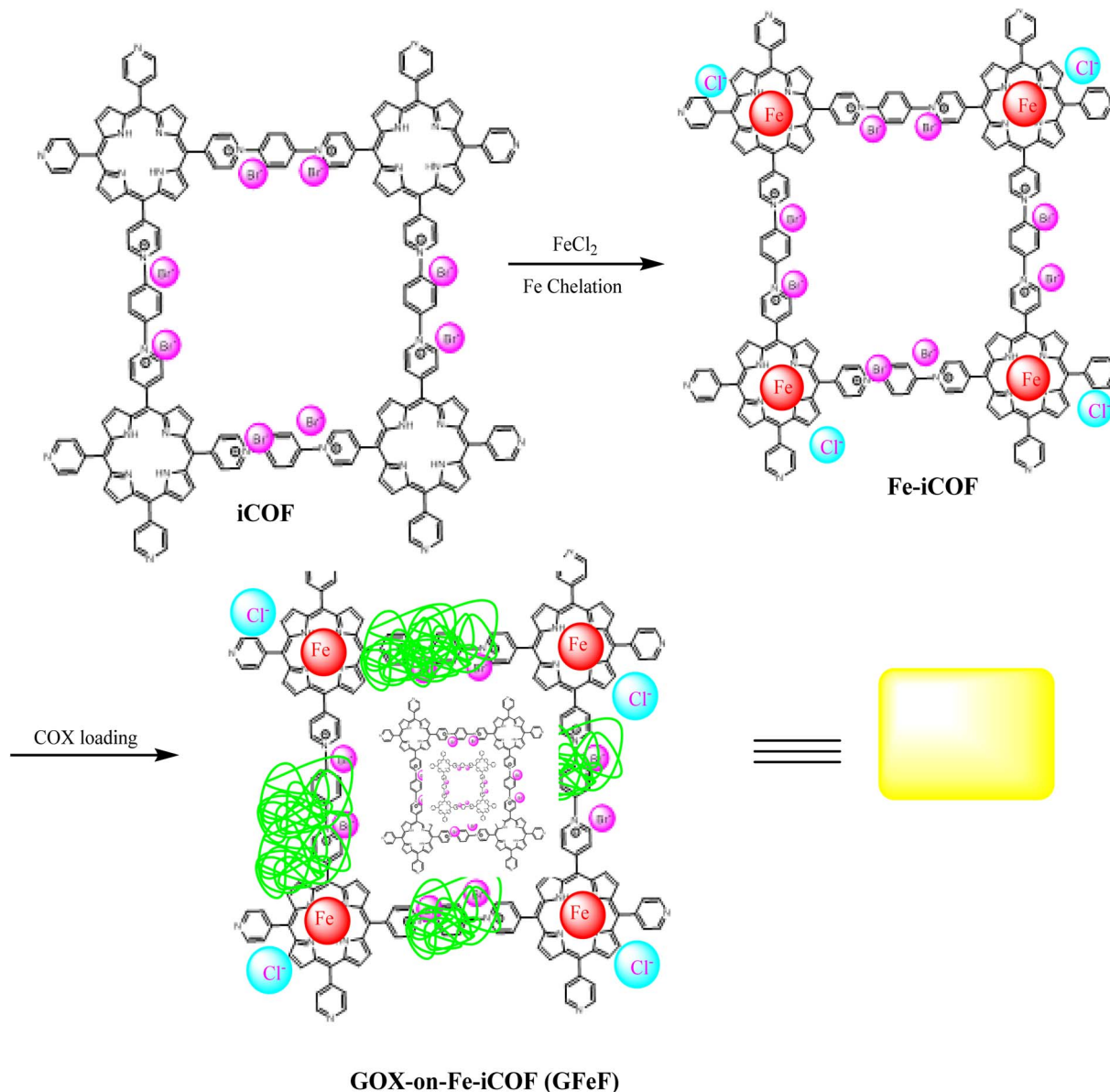


Fig. 13 The preparation of GOX-on-Fe-iCOF (GFeF) nanzyme. Reproduced with permission from ref. 48.

was centrifuged with glucose oxidase (GOX) to produce the final GFeF nanzyme.<sup>48</sup> Through the electrostatic interactions, GOX was loaded on the surface of GFeF for catalyzing the conversion of glucose to gluconic acid and  $\text{H}_2\text{O}_2$  by oxygen. Chelated porphyrin-based iCOF (Fe-iCOF) was incorporated with Fe ions with peroxidase action to convert  $\text{H}_2\text{O}_2$  to hydroxyl radicals with oxidizing activities; accordingly, glucose turned to gluconic acid and  $\text{H}_2\text{O}_2$  for wound healing (Fig. 13).<sup>48</sup> It was found that *E. coli* and *S. aureus* still sustain the unique round and rod structure, which showed that glucose or GFeF have less toxicity for bacteria. Although, the bacterial structure was deformed in glucose and GFeF, GFeF was adsorbed on the outer surfaces of bacteria, and condenses the diffuse distance-shaped  $\cdot\text{OH}$  radicals and bacteria, which kills bacteria efficiently. It was proven by studying the main organs of the mice wherein Fe-iCOF-Gel and GFeF-Gel bandages did not yield acute toxicity to the mice (Fig. 14).<sup>48</sup>

### 3.8. Covalent organic nanosheets (CONs) with antimicrobial effects

2D covalent organic nanosheets (CONs) were designed for capturing the phosphate ions from  $\text{H}_2\text{O}$  using porous and self-exfoliative pyrene-based guanidine-containing CONs by

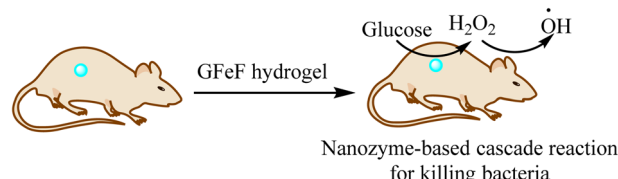


Fig. 14 The mechanism of GOX-on-Fe-iCOF (GFeF) nanzyme. Reproduced with permission from ref. 48.

removing the phosphate as oxoanions in  $\text{H}_2\text{O}$ . Notably, these materials could remove the phosphates from  $\text{H}_2\text{O}$  to obtain antimicrobial properties contrary to the pathogenic and antibiotic-resistant bacteria.<sup>90,91</sup> In addition, a CON-based system was introduced with stronger hydrogen bonding between guanidine and phosphate ions, displaying similar adsorption capability towards phosphate ions (below pH 8.0) and providing a much lower adsorption capacity (over pH 10); this water-insoluble amorphous polymer with good recyclability could efficiently desorb and recover these phosphate ions. On the other hand, guanidine-containing CONs can be deployed against antibiotic-resistant bacteria, paving a way for designing novel antibacterial systems with both water treatment/remediation and antibacterial applicability (Fig. 15).<sup>92</sup>

### 3.9. COF-based systems with photodynamic, photothermal, and nanozymatic activities

The design of the conjugated COFs with photodynamic and photothermal activities against bacterial infections and drug-

resistant bacteria has been investigated. In terms of antibiotic-resistant bacteria, phototherapeutic techniques deploying these structures can be considered as promising tactics, especially for chronic wound healing and bacterial infections (diabetic wounds). For instance, under the single NIR irradiation, (5,10,15,20-tetrakis(4-aminophenyl)-21*H*,23*H*-porphine)-(10-(4-chlorophenyl)-5,5-difluoro-2,8-diformyl-1,3,7,9-tetramethyl-5*H*-dipyrrolo-[1,2-c:2',1'-f][1,3,2]diazaborinin-4-iium-5-uide) TAPP-BDP acted as a triple bacterial inhibitory agent, providing synergistic photothermal, photodynamic, and peroxidase performances. The long  $\pi$ -conjugated structure of TAPP-BDP could enhance the absorption in NIR; the photothermal effect increased the temperature to afford bacterial collapse. Accordingly, it exhibited efficient antibacterial activities towards Gram-negative and positive pathogenic and drug-resistant bacteria (Fig. 16).<sup>93</sup>

5,10,15,20-Tetrakis(4-aminophenyl)-21*H*,23*H*-porphine (TAPP) and 10-(4-chlorophenyl)-5,5-difluoro-2,8-diformyl-1,3,7,9-tetramethyl-5*H*-dipyrrolo-[1,2-c:2',1'-f][1,3,2]diazaborinin-4-iium-5-uide

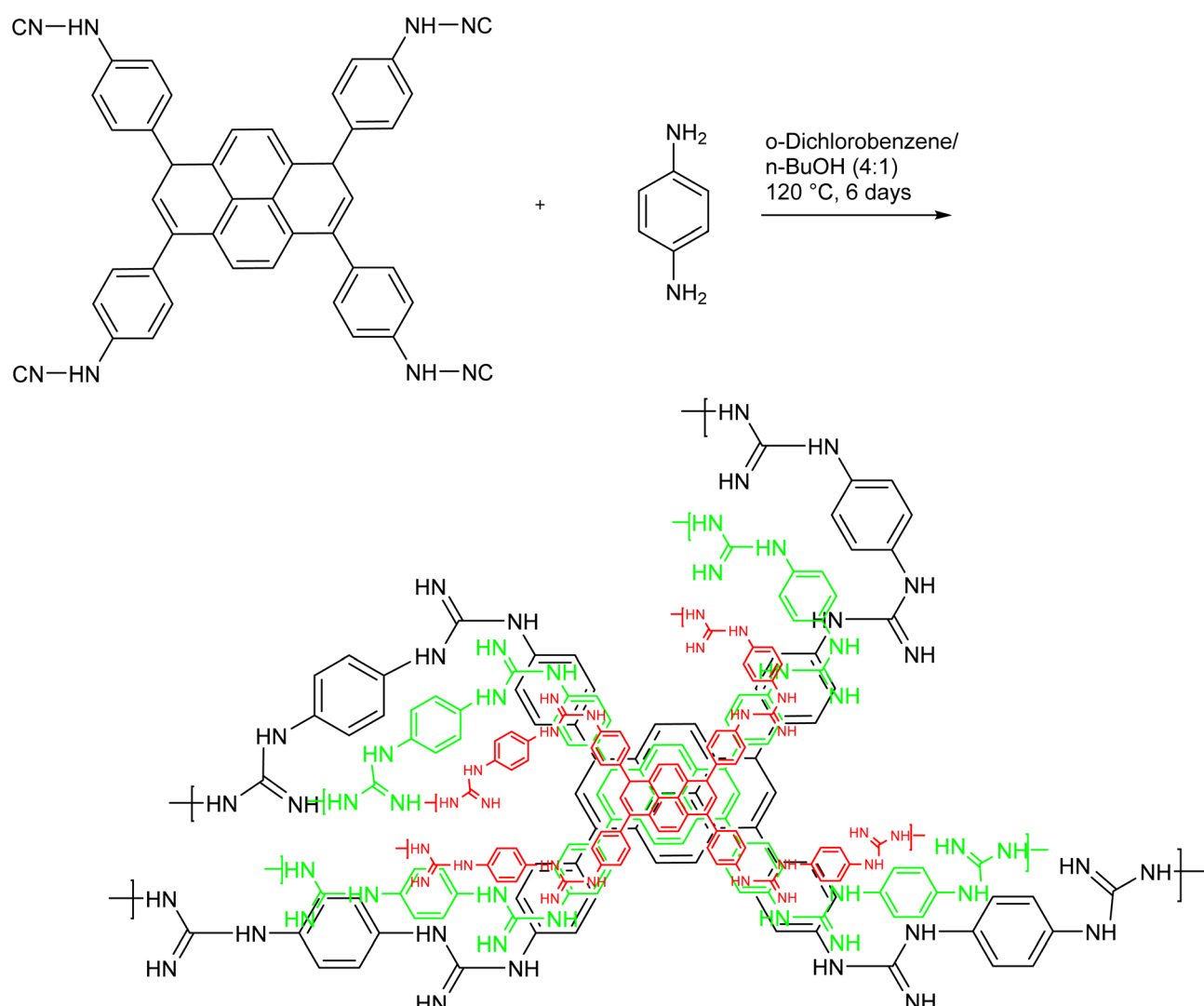


Fig. 15 The preparative process of guanidine-containing CONs. Reproduced with permission from ref. 92.



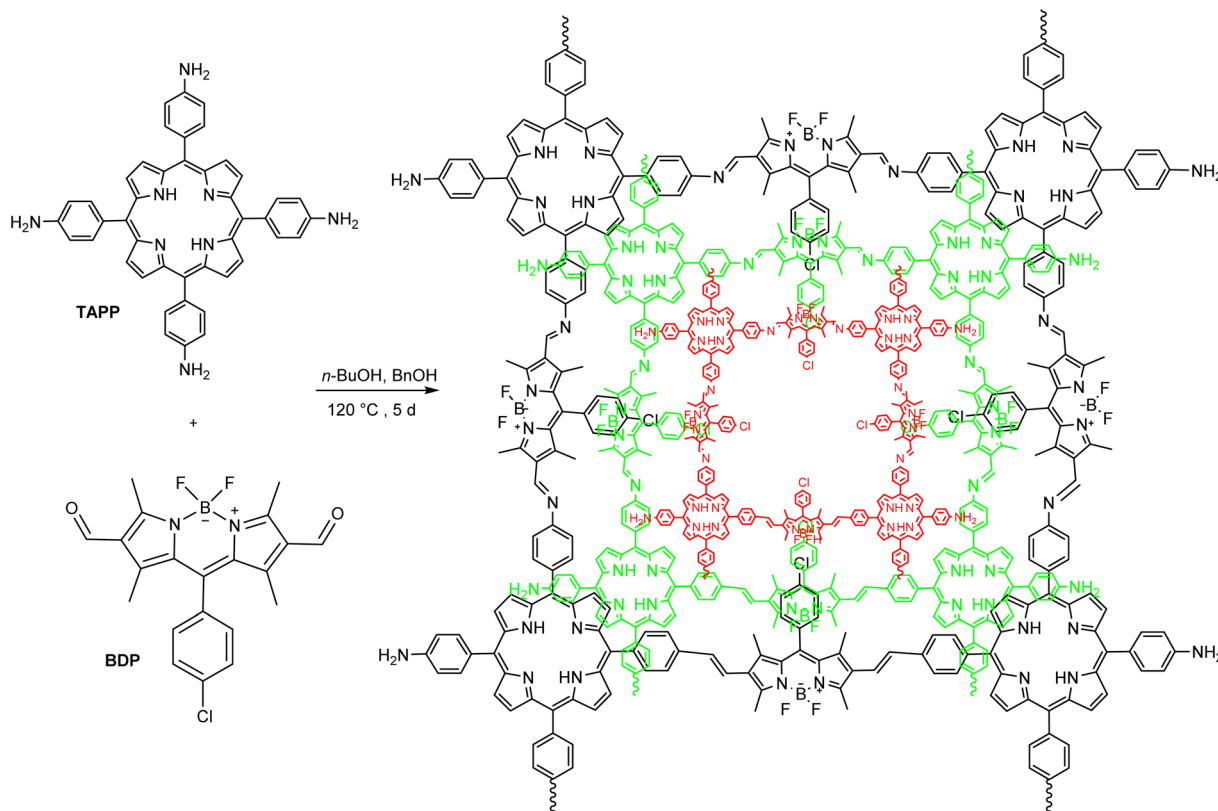


Fig. 16 The preparative process of the TAPP–BDP. Reproduced with permission from ref. 93.

(BDP) were reacted to generate a photosensitive COF (TAPP–BDP) that offers photodynamic/photothermal/nanozymatic antibacterial treatment under a single NIR light radiation. The higher lengthy  $\pi$  conjugated structure (TAPP–BDP) with photodynamic possessions and photothermal alteration was constructed; the POD action of TAPP–BDP catalyzed  $\text{H}_2\text{O}_2$  to toxic 'OH for killing bacteria in an acidic microenvironment.<sup>94,95</sup> Thus, it could be employed for promoting wound healing as an antibacterial infection agent. To evaluate the mechanism of TAPP–BDP, terephthalic acid (TA) as the nonfluorescent compound and EPR were applied to observe the formation of 'OH. It was found that fluorescence was enhanced by TAPP–BDP,  $\text{H}_2\text{O}_2$ , and TA under NIR light illumination, implying that the POD (peroxidase) activity of TAPP–BDP turning  $\text{H}_2\text{O}_2$  to 'OH (Fig. 17).<sup>93</sup>

### 3.10. Synthesis of imine-linked COF with antibacterial effects

Imine-linked COFs were fabricated by the treatment of terephthalaldehyde with diethylenetriamine utilizing the acetic acid as a catalyst in dioxane, providing the COF with higher sensitivity counter to diverse antibacterial infections.<sup>96</sup> This product revealed efficient antibacterial activities (Fig. 18).<sup>96</sup> Also, electrostatic interactions and hydrogen bonds were realized as the mechanisms for the adsorption of bacteria by imine-linked COF. On the other hand, there are some ways to kill bacteria such as *via* hydrophobic bonds, coordination bonds, and adsorption concentration causing precipitation and coagulation of cytoplasmic proteins. The stability assessments of imine-linked COFs was studied in  $\text{CHCl}_3$ ,

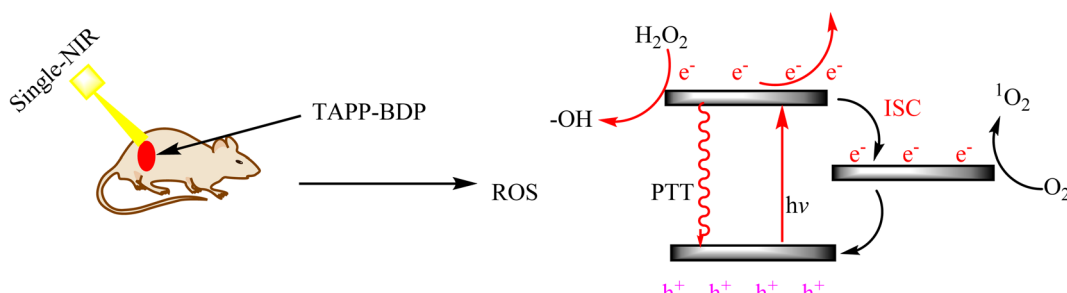


Fig. 17 Mechanism of TAPP–BDP. Reproduced with permission from ref. 93.



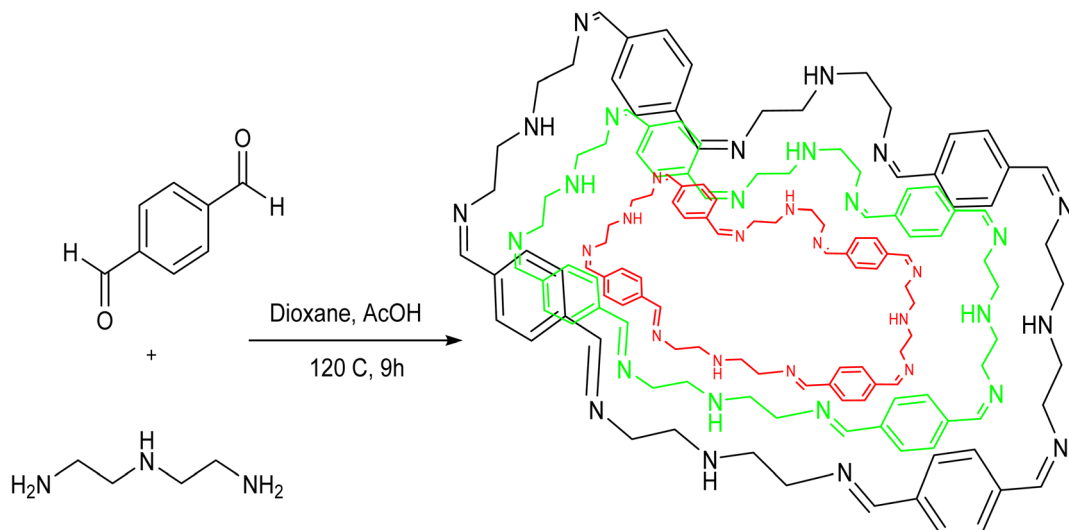


Fig. 18 The preparative process of COF-TDETA. Reproduced with permission from ref. 96.

$\text{H}_2\text{O}$ ,  $\text{HCl}$ , and  $\text{NaOH}$ . Accordingly, it was found that imine-linked COFs were stable in water, chloroform, and sodium hydroxide. However, the imine linkage poses a fundamental limitation due to its low stability under harsh conditions and its inappropriateness for in-plane *p*-conjugation in COFs.<sup>96</sup>

### 3.11. Benzoxazine-linked COFs with antimicrobial effects

Novel hydroxyl-covering imine-linked 2D COFs were fabricated through a solvothermal synthesis technique, showing efficient antibacterial effects; the pore structure was retained for the controlled drug delivery and release. These benzoxazine-linked

Table 1 Some selected examples of COFs-based materials for wound healing and antibacterial applications

COF-based materials	Advantages/properties	Ref.
CUR@COF/PCL NFM	<ul style="list-style-type: none"> <li>Suitable thermal and mechanical stability</li> <li>Antibacterial and antioxidant properties</li> <li>Release of CUR by Fickian diffusion</li> <li>Low cytotoxicity and good biocompatibility</li> </ul>	77
IBU@DhaTph- membrane	<ul style="list-style-type: none"> <li>Efficient antibacterial and anti-inflammatory effects</li> <li>Effects <i>via</i> (<math>\text{O}_2</math>) generation and manageable IBU release</li> <li>Anti-infection and tissue renovation actions</li> </ul>	81
NMC <sub>Tp-TTA</sub> hybrid nanzyme	<ul style="list-style-type: none"> <li>Efficiency peroxidase mimic</li> <li>The conjugation effects of COFs and light harvesting</li> </ul>	22
Acridine-based COF	<ul style="list-style-type: none"> <li>Efficient antibacterial activity</li> </ul>	85
ENR-FM-COF-TPU	<ul style="list-style-type: none"> <li>Antibacterial effects against <i>S. aureus</i> and <i>E. coli</i></li> <li>Physicochemical and biological possessions</li> <li>Morphology, correct hydrophobicity</li> <li>Water uptake capacity and biocompatibility</li> <li>Killing <i>E. coli</i> and <i>S. aureus</i> (<i>in vitro</i>)</li> <li>Good biocompatibility with improved biodegradability</li> <li>Suitable anti-inflammatory effects with low phototoxicity</li> <li>Superb wound healing effects (<i>in vivo</i>)</li> </ul>	87
TP-Por-CON	<ul style="list-style-type: none"> <li>Killing <i>E. coli</i> and <i>S. aureus</i> (<i>in vitro</i>)</li> <li>Good biocompatibility with improved biodegradability</li> <li>Suitable anti-inflammatory effects with low phototoxicity</li> <li>Superb wound healing effects (<i>in vivo</i>)</li> </ul>	83
GOX-on-Fe-iCOF (GFeF) nanzyme	<ul style="list-style-type: none"> <li>Antibacterial result</li> <li>Good biocompatibility</li> </ul>	48
2D-g-CONs	<ul style="list-style-type: none"> <li>Rapid and efficient elimination of phosphates</li> <li>The antibacterial activities against <i>E. coli</i>, <i>S. aureus</i>, and MRSA</li> </ul>	92
TAPP-BDP construction	<ul style="list-style-type: none"> <li>Low toxicity and respectable biocompatibility</li> <li>Antibacterial efficiency</li> <li>Antibacterial effects against <i>S. aureus</i> in living organisms under a single NIR light radiation</li> </ul>	93
COF-TDETA	<ul style="list-style-type: none"> <li>Thermal and chemical constancy</li> <li>It can be applied against <i>S. aureus</i>, <i>Enterococcus faecalis</i>, <i>E. coli</i>, and <i>Pseudomonas aeruginosa</i></li> <li>Antibacterial effects against antibiotic-resistant bacteria such as <i>E. coli</i> and <i>S. aureus</i></li> <li>Non-toxicity, excellent thermal stability, biocompatibility, manageable pore size</li> </ul>	96
TAPT-DHNDA-Ba-COF-B	<ul style="list-style-type: none"> <li><math>\text{CO}_2</math> and <math>\text{N}_2</math> could be eliminated using this benzoxazine-linked COF with efficient gas adsorption capacity</li> </ul>	76

COFs with antibacterial effects could be obtained after the post-synthetic modification procedures. 2,4,6-tris(4-aminophenyl)-1,3,5-triazine (TAPT) was added to 2,6-dihydroxynaphthalene-1,5-dicarbaldehyde (DHNDA) in 1,3,5-trimethylbenzene and 1,4-dioxane with acetic acid to provide TAPT-DHNDA-COF. Subsequently, it was reduced by  $\text{NaBH}_4$  to provide TAPT-DHNDA-BH-COF, followed by the reaction with formaldehyde solution in  $\text{CH}_2\text{Cl}_2$  to offer TAPT-DHNDA-Ba-COF-F, which was reacted with benzaldehyde to produce TAPT-DHNDA-Ba-COF-B.<sup>90,97</sup> The mechanism was associated with the inhibition of bacterial DNA replication. The antibacterial analyses revealed that the characteristic peak of benzoxazine-linked COF still existed, showing a decent antibacterial activity; the inhibition rate was  $\sim 99\%$ . Thus, this material can be considered a promising agent with potential antibacterial effects in biomedicine.<sup>90,97</sup> Analysis of biosafety issues as well as clinical translation studies ought to be crucial criteria for future explorations. Undoubtedly, COFs with intrinsic features of suitable size, modular pore geometry and porosity, and straightforward post-synthetic modification through simple organic transformations, are attractive candidates for designing various advanced (nano)systems for wound healing/dressing and antibacterial drug delivery. Besides, in some cases like triazine-based COFs, they can be applied as photosensitizers for the photodynamic inactivation of bacteria.<sup>98</sup> The capability of COFs to disintegrate in a slightly acidic tumor microenvironment offers the advantage of targeted delivery.<sup>99</sup> However, more elaborative studies are still required pertaining to the synthesis of COFs and identification of optimal conditions. On the other hand, nanotoxicological assessments are crucial aspects in clinical and biomedical applications of nanomaterials, since they may cause possible harmful or toxic effects on human health or the environments.<sup>100</sup> For instance, oxidative stress responses ensuing from ROS generation are one of the most frequent nanomaterial-based toxicities; it may additionally stimulate pathophysiological impacts, including inflammation, fibrosis, and genotoxicity.<sup>101</sup> Thus, more elaborative studies should be focused on pre-clinical and pharmacological assessments as well as biosafety and toxicological analyses. To better compare the COF-based systems designed for wound healing and antimicrobial applications, some salient advantages, and properties of them are summarized in Table 1.

## 4. Conclusions and perspectives

Drug-loaded COFs can be deployed for antibacterial photocatalytic therapy. A variety of complex COF-based structures (e.g., acridine-based COFs) have been designed to afford high singlet oxygen ( ${}^1\text{O}_2$ ) at body temperature, serving as antibacterial agents under visible light. COFs as porous materials can be applied for the targeted drug delivery with controlled release behavior against chronic and resistant bacterial infections. Wound-healing drugs could be loaded on these mesoporous COF-based materials using different approaches. Studies on *in vitro* or *in vivo* drug release have been performed in diverse pH ranges to evaluate the release behavior of COF-based systems. Controlled drug delivery can be achieved against bacterial

infections by loading the drug or  ${}^1\text{O}_2$  via the photocatalytic generation by thermo-responsive pathways. As highlighted in this review, efficient wound healing can be obtained using drug-loaded COFs or  ${}^1\text{O}_2$  generated by them. The relatively inexpensive sources and reduced time required for wound healing have received noteworthy attention. It is expected that diverse strategies incorporating COFs can be designed in the future to provide novel and imaginative disease treatment strategies.

There are some limitations regarding the applications of COF-based structures, which have not been considered enough. Consequently, forthcoming policies should be focused on morphologies with shared complementarity to improve their properties and applications. For example, positively charged zero-dimensional (0-D) COF nanospheres confirmed the well-organized adsorption of negative elements. The 2-D COF films are size-selective molecular separation dependent on the COF's diameters. As such, a mixture of 0-D COF nanospheres and 2-D COF thin films by the layer-by-layer sandwich structure were utilized for the choosy separation of minor cationic molecules. This outlook review highlights synthetic approaches and improved settings for creating COF nano morphologies in all dimensions. The incorporation of the COF with their physical orderliness, precise surface area, and chemical functionalities, has vital characteristics in their performance in numerous applications such as adsorption, separation, storage, ion exchange, drug delivery, ion transport, heterogeneous catalysis, sensors, and water harvesting.

## Abbreviation

TMB	Tetramethylbenzidine
$\text{FeCl}_3 \cdot 6\text{H}_2\text{O}$	Iron chloride hexahydrate
TTA	4,4',4''-(1,3,5-triazine-2,4,6-triyl)trianiline
Tp	1,3,5-Triformylphloroglucinol
TFB	Benzene-1,3,5-tricarboxaldehyde
TAPB	1,3,5-Tris(4-aminophenyl)benzene
DMF	<i>N,N</i> -Dimethylformamide
DAA	Proflavine named 3,6-diaminoacridine
PCL	Polycaprolactone
APCT	Antibacterial photocatalytic therapy
DMTA	2,5-Dimethoxyterephthalaldehyde
TPyP	5,10,15,20-Tetra(4-pyridyl)-21H,23H-porphine
BNN6	<i>N,N'</i> -di-sec-butyl- <i>N,N'</i> -dinitroso-1,4-phenylenediamine
NMP	1-Methyl-2-pyrrolidinone
TPyP	5,10,15,20-Tetra(4-pyridyl)-21H,23H-porphine
2-NH <sub>2</sub> -BDC	2-Aminoterephthalic acid
COFs	Covalent organic frameworks
GOX	Glucose oxidase
TFP	2,4,6-Triformylphloroglucinol
Tph a	5,10,15,20-tetrakis(4-aminophenyl)porphyrin
CUR	Curcumin

## Conflicts of interest

There are no conflicts of interest.



## Acknowledgements

We are grateful for the Research Council's support of Alzahra University.

## References

- H. Goesmann and C. Feldmann, *Angew. Chem., Int. Ed.*, 2010, **49**, 1362–1395.
- R. Jin, C. Zeng, M. Zhou and Y. Chen, *Chem. Rev.*, 2016, **116**, 10346–10413.
- H. Furukawa, K. E. Cordova, M. O'Keeffe and O. M. Yaghi, *Science*, 2013, **341**, 1230444.
- S. Horike, S. Shimomura and S. Kitagawa, *Nat. Chem.*, 2009, **1**, 695–704.
- H.-C. Zhou, J. R. Long and O. M. Yaghi, *Chem. Rev.*, 2012, **112**, 673–674.
- Z. Chen, K. O. Kirlikovali, P. Li and O. K. Farha, *Acc. Chem. Res.*, 2022, **55**, 579–591.
- A. Ejsmont, J. Andreo, A. Lanza, A. Galarda, L. Macreadie, S. Wuttke, S. Canossa, E. Ploetz and J. Goscianska, *Coord. Chem. Rev.*, 2021, **430**, 213655.
- C. Diercks and O. Yaghi, *Science*, 2017, 355.
- H. Wang, Z. Zeng, P. Xu, L. Li, G. Zeng, R. Xiao, Z. Tang, D. Huang, L. Tang and C. Lai, *Chem. Soc. Rev.*, 2019, **48**, 488–516.
- M. S. Lohse and T. Bein, *Adv. Funct. Mater.*, 2018, **28**, 1870229.
- S. J. Lyle, P. J. Waller and O. M. Yaghi, *Trends Chem.*, 2019, **1**, 172–184.
- T. T. M. Nguyen, H. M. Le, Y. Kawazoe and H. L. Nguyen, *Mater. Chem. Front.*, 2018, **2**, 2340.
- H. Yazdani, M.-A. Shahbazi and R. S. Varma, *ACS Appl. Bio Mater.*, 2022, **51**, 40–58.
- K. Geng, T. He, R. Liu, S. Dalapati, K. T. Tan, Z. Li, S. Tao, Y. Gong, Q. Jiang and D. Jiang, *Chem. Rev.*, 2020, **120**, 8814–8933.
- S. Liu, J. Yang, R. Guo, L. Deng, A. Dong and J. Zhang, *Macromol. Rapid Commun.*, 2020, **41**, 1900570.
- X. Wang, X. Han, J. Zhang, X. Wu, Y. Liu and Y. Cui, *J. Am. Chem. Soc.*, 2016, **138**, 12332–12335.
- S. Liu, C. Hu, Y. Liu, X. Zhao, M. Pang and J. Lin, *Chem.-Eur. J.*, 2019, **25**, 4315–4319.
- L. Zhang, S. Wang, Y. Zhou, C. Wang, X. Z. Zhang and H. Deng, *Angew. Chem., Int. Ed.*, 2019, **58**, 14213–14218.
- Y. Peng, Y. Huang, Y. Zhu, B. Chen, L. Wang, Z. Lai, Z. Zhang, M. Zhao, C. Tan and N. Yang, *J. Am. Chem. Soc.*, 2017, **139**, 8698–8704.
- S. Yan, X. Guan, H. Li, D. Li, M. Xue, Y. Yan, V. Valtchev, S. Qiu and Q. Fang, *J. Am. Chem. Soc.*, 2019, **141**, 2920–2924.
- R. K. Sharma, P. Yadav, M. Yadav, R. Gupta, P. Rana, A. Srivastava, R. Zbořil, R. S. Varma, M. Antonietti and M. B. Gawande, *Mater. Horiz.*, 2020, **7**, 411–454.
- L. Zhang, Z. Liu, Q. Deng, Y. Sang, K. Dong, J. Ren and X. Qu, *Angew. Chem., Int. Ed.*, 2021, **60**, 3469–3474.
- E. Martínez-Periñán, M. Martínez-Fernández, J. L. Segura and E. Lorenzo, *Sensors*, 2022, **22**, 4758.
- A. Schlachter, P. Asselin and P. D. Harvey, *ACS Appl. Mater. Interfaces*, 2021, **13**, 26651–26672.
- C. Dwivedi, H. Pandey, A. C. Pandey, S. Patil, P. W. Ramteke, P. Laux, A. Luch and A. V. Singh, *Pharmaceutics*, 2019, **11**, 180.
- X. Dai, Q. Guo, Y. Zhao, P. Zhang, T. Zhang, X. Zhang and C. Li, *ACS Appl. Mater. Interfaces*, 2016, **8**, 25798–25807.
- T. Wei, Z. Tang, Q. Yu and H. Chen, *ACS Appl. Mater. Interfaces*, 2017, **9**, 37511–37523.
- X. Feng, X. Ding and D. Jiang, *Chem. Soc. Rev.*, 2012, **41**, 6010–6022.
- Q. Guan, L.-L. Zhou, W.-Y. Li, Y.-A. Li and Y.-B. Dong, *Chem.-Eur. J.*, 2020, **26**, 5583–5591.
- Y. Zhang, H. Liu, F. Gao, X. Tan, Y. Cai, B. Hu, Q. Huang, M. Fang and X. Wang, *EnergyChem*, 2022, 100078.
- P. J. Waller, F. Gádara and O. M. Yaghi, *Acc. Chem. Res.*, 2015, **48**, 3053–3063.
- L. Bai, S. Z. F. Phua, W. Q. Lim, A. Jana, Z. Luo, H. P. Tham, L. Zhao, Q. Gao and Y. Zhao, *Chem. Commun.*, 2016, **52**, 4128–4131.
- G. Chedid and A. Yassin, *Nanomaterials*, 2018, **8**, 916.
- Q. Fang, J. Wang, S. Gu, R. B. Kaspar, Z. Zhuang, J. Zheng, H. Guo, S. Qiu and Y. Yan, *J. Am. Chem. Soc.*, 2015, **137**, 8352–8355.
- Q. Guan, L. L. Zhou, W. Y. Li, Y. A. Li and Y. B. Dong, *Chem.-Eur. J.*, 2020, **26**, 5583–5591.
- G. Zhang, X. Li, Q. Liao, Y. Liu, K. Xi, W. Huang and X. Jia, *Nat. Commun.*, 2018, **9**(1), 2785.
- G. C. Gurtner, S. Werner, Y. Barrandon and M. T. Longaker, *Nature*, 2008, **453**, 314–321.
- A. A. Ross, A. Rodrigues Hoffmann and J. D. Neufeld, *Microbiome*, 2019, **7**, 79.
- A. V. Nguyen and A. M. Soulika, *Int. J. Mol. Sci.*, 2019, **20**, 1811.
- H. Cortes, I. H. Caballero-Florán, N. Mendoza-Muñoz, E. N. Córdova-Villanueva, L. Escutia-Guadarrama, G. Figueroa-González, O. D. Reyes-Hernández, M. González-Del Carmen, M. Varela-Cardoso and J. J. Magaña, *Cell. Mol. Biol.*, 2020, **66**, 191–198.
- J. S. Boateng, K. H. Matthews, H. N. Stevens and G. M. Eccleston, *J. Pharm. Sci.*, 2008, **97**, 2892–2923.
- S. Dhivya, V. V. Padma and E. Santhini, *BioMedicine*, 2015, **5**(4), 24–28.
- M. Haalboom, *Curr. Med. Chem.*, 2018, **25**, 5772–5781.
- D. W.-C. Chen and S.-J. Liu, *Nanomedicine*, 2015, **10**, 1959–1971.
- X. Hu, S. Liu, G. Zhou, Y. Huang, Z. Xie and X. Jing, *J. Controlled Release*, 2014, **185**, 12–21.
- J.-I. Alos, *Enferm. Infect. Microbiol. Clin.*, 2014, **33**, 692–699.
- J. Davies and D. Davies, *Microbiol. Mol. Biol. Rev.*, 2010, **74**, 417–433.
- Y. Li, L. Wang, H. Liu, Y. Pan, C. Li, Z. Xie and X. Jing, *Small*, 2021, **17**, 2100756.
- G. Taubes, *Science*, 2008, 356–361.
- G. D. Wright, *Nat. Rev. Microbiol.*, 2007, **5**, 175–186.
- Z. Chen, Z. Wang, J. Ren and X. Qu, *Acc. Chem. Res.*, 2018, **51**, 789–799.



52 L. Wang, W. Yang, W. Zhu, X. Guan, Z. Xie and Z.-M. Sun, *Inorg. Chem.*, 2014, **53**, 11584–11588.

53 Y. Li, K. Fukushima, D. J. Coady, A. C. Engler, S. Liu, Y. Huang, J. S. Cho, Y. Guo, L. S. Miller and J. P. Tan, *Angew. Chem., Int. Ed.*, 2013, **52**, 674–678.

54 W. Y. Chen, H. Y. Chang, J. K. Lu, Y. C. Huang, S. G. Harroun, Y. T. Tseng, Y. J. Li, C. C. Huang and H. T. Chang, *Adv. Funct. Mater.*, 2015, **25**, 7189–7199.

55 A. Muñoz-Bonilla and M. Fernández-García, *Prog. Polym. Sci.*, 2012, **37**, 281–339.

56 A. P. West, I. E. Brodsky, C. Rahner, D. K. Woo, H. Erdjument-Bromage, P. Tempst, M. C. Walsh, Y. Choi, G. S. Shadel and S. Ghosh, *Nature*, 2011, **472**, 476–480.

57 Y. Liao, J. Li and A. Thomas, *ACS Macro Lett.*, 2017, **6**, 1444–1450.

58 Y. Zhi, P. Shao, X. Feng, H. Xia, Y. Zhang, Z. Shi, Y. Mu and X. Liu, *J. Mater. Chem. A*, 2018, **6**, 374–382.

59 S. Dalapati, E. Jin, M. Addicoat, T. Heine and D. Jiang, *J. Am. Chem. Soc.*, 2016, **138**, 5797–5800.

60 S.-Y. Yu, J. Mahmood, H.-J. Noh, J.-M. Seo, S.-M. Jung, S.-H. Shin, Y.-K. Im, I.-Y. Jeon and J.-B. Baek, *Angew. Chem., Int. Ed.*, 2018, **57**, 8438–8442.

61 A. P. Côté, A. I. Benin, N. W. Ockwig, M. O'Keeffe, A. J. Matzger and O. M. Yaghi, *Science*, 2005, **310**, 1166–1170.

62 H. M. El-Kaderi, J. R. Hunt, J. L. Mendoza-Cortés, A. P. Côté, R. E. Taylor, M. O'Keeffe and O. M. Yaghi, *Science*, 2007, **316**, 268–272.

63 M. S. Lohse and T. Bein, *Adv. Funct. Mater.*, 2018, **28**, 1705553.

64 H. R. Abuzeid, A. F. M. El-Mahdy and S.-W. Kuo, *Giant*, 2021, **6**, 100054.

65 W. Li, C.-X. Yang and X.-P. Yan, *Chem. Commun.*, 2017, **53**, 11469–11471.

66 X. Guan, Q. Fang, Y. Yan and S. Qiu, *Acc. Chem. Res.*, 2022, **55**, 1912–1927.

67 J. C. Beard and T. M. Swager, *J. Org. Chem.*, 2021, **86**, 2037–2057.

68 Y. Zhang, Y.-G. Zhao, N. Muhammad, M.-L. Ye and Y. Zhu, *J. Chromatogr. A*, 2020, **1618**, 460891.

69 P. Yadav, M. Yadav, R. Gaur, R. Gupta, G. Arora, A. Srivastava, A. Goswami, M. B. Gawande and R. K. Sharma, *Mater. Adv.*, 2022, **3**, 1432–1458.

70 Y. Zhang, Y.-G. Zhao, N. Muhammad, M.-L. Ye and Y. Zhu, *J. Chromatogr. A*, 2020, **1618**, 460891.

71 F. Gorky, A. Nambo and M. L. Carreon, *J. CO<sub>2</sub> Util.*, 2021, **51**, 101642.

72 Z. Chen and R. L. Valentine, *Environ. Sci. Technol.*, 2008, **42**, 5062–5067.

73 S. Kumar, G. Ignacz and G. Szekely, *Green Chem.*, 2021, **23**, 8932–8939.

74 C. Zhu, S. Pang, Z. Chen, L. Bi, S. Wang, C. Liang and C. Qin, *Polymers*, 2022, **14**, 3158.

75 F. Mohajer, G. Mohammadi Ziarani and A. Badiei, *RSC Adv.*, 2021, **11**, 6517–6525.

76 G. Mohammadi Ziarani, P. Mofatehnia, F. Mohajer and A. Badiei, *RSC Adv.*, 2020, **10**, 30094–30109.

77 Y. Zou, P. Wang, A. Zhang, Z. Qin, Y. Li, Y. Xianyu and H. Zhang, *ACS Appl. Mater. Interfaces*, 2022, **14**, 8680–8692.

78 C. De Savi, R. H. Bradbury, A. A. Rabow, R. A. Norman, C. de Almeida, D. M. Andrews, P. Ballard, D. Buttar, R. J. Callis and G. S. Currie, *J. Med. Chem.*, 2015, **58**, 8128–8140.

79 Q. Guan, L.-L. Zhou, Y.-A. Li, W.-Y. Li, S. Wang, C. Song and Y.-B. Dong, *ACS Nano*, 2019, **13**, 13304–13316.

80 S. Liu, C. Hu, Y. Liu, X. Zhao, M. Pang and J. Lin, *Chem.-Eur. J.*, 2019, **25**, 4315–4319.

81 L.-G. Ding, S. Wang, B.-J. Yao, F. Li, Y.-A. Li, G.-Y. Zhao and Y.-B. Dong, *Adv. Healthcare Mater.*, 2021, **10**, 2001821.

82 S. Bauer, C. Serre, T. Devic, P. Horcajada, J. Marrot, G. Férey and N. Stock, *Inorg. Chem.*, 2008, **47**, 7568–7576.

83 B. Sun, Z. Ye, M. Zhang, Q. Song, X. Chu, S. Gao, Q. Zhang, C. Jiang, N. Zhou and C. Yao, *ACS Appl. Mater. Interfaces*, 2021, **13**, 42396–42410.

84 C. Zhang, J. Guo, X. Zou, S. Guo, Y. Guo, R. Shi and F. Yan, *Adv. Health Mater.*, 2021, **10**, e2100775.

85 M. K. Gatasheh, S. Kannan, K. Hemalatha and N. Imrana, *Karbala Int. J. Mod. Sci.*, 2017, **3**, 272–278.

86 Y. Zhang, M. Luo, Y. Zu, Y. Fu, C. Gu, W. Wang, L. Yao and T. Efferth, *Chem.-Biol. Interact.*, 2012, **199**, 129–136.

87 C. Li, C. Chen, J. Zhao, M. Tan, S. Zhai, Y. Wei, L. Wang and T. Dai, *ACS Biomater. Sci. Eng.*, 2021, **7**, 3898–3907.

88 R. Q. Wang, X. B. Wei and Y. Q. Feng, *Chem.-Eur. J.*, 2018, **24**, 10979–10983.

89 H. Wang, X. Cai, Y. Zhang, T. Zhang, M. Chen, H. Hu, Z. Huang, J. Liang and Y. Qin, *Appl. Surf. Sci.*, 2021, **555**, 149708.

90 Z.-l. Tang, Z.-w. Xia, S.-h. Chang and Z.-x. Wang, *Bioorg. Med. Chem. Lett.*, 2015, **25**, 3378–3381.

91 S. Mitra, S. Kandambeth, B. P. Biswal, A. Khayum M, C. K. Choudhury, M. Mehta, G. Kaur, S. Banerjee, A. Prabhune, S. Verma, S. Roy, U. K. Kharul and R. Banerjee, *J. Am. Chem. Soc.*, 2016, **138**, 2823–2828.

92 S. Dey, S. Das, A. Patel, K. V. Raj, K. Vanka and D. Manna, *J. Mater. Chem. A*, 2022, **10**, 4585–4593.

93 G.-P. Yang, X.-L. Meng, S.-J. Xiao, Q.-Q. Zheng, Q.-G. Tan, R.-P. Liang, L. Zhang, P. Zhang and J.-D. Qiu, *ACS Appl. Mater. Interfaces*, 2022, **24**, 28289–28300.

94 F. Cao, L. Zhang, H. Wang, Y. You, Y. Wang, N. Gao, J. Ren and X. Qu, *Angew. Chem., Int. Ed.*, 2019, **58**, 16236–16242.

95 S. Wu, C. Xu, Y. Zhu, L. Zheng, L. Zhang, Y. Hu, B. Yu, Y. Wang and F.-J. Xu, *Adv. Funct. Mater.*, 2021, **31**, 2103591.

96 E. A. Gendy, A. I. Khodair, A. M. Fahim, D. T. Oyekunle and Z. Chen, *J. Mol. Liq.*, 2022, **358**, 119191.

97 E. A. Gendy, D. T. Oyekunle, J. Ifthikar, A. Jawad and Z. Chen, *Environ. Sci. Pollut. Res.*, 2022, **29**, 32566–32593.

98 T. Liu, X. Hu, Y. Wang, L. Meng, Y. Zhou, J. Zhang, M. Chen and X. Zhang, *J. Photochem. Photobiol. B*, 2017, **175**, 156–162.

99 N. Singh, J. Kim, J. Kim, K. Lee, Z. Zunbul, I. Lee, E. Kim, S.-G. Chi and J. S. Kim, *Bioact. Mater.*, 2023, **21**, 358–380.

100 Y.-C. Chen, K.-Y. A. Lin, K.-F. Chen, X.-Y. Jiang and C.-H. Lin, *Environ. Pollut.*, 2021, **273**, 116528.

101 A. Manke, L. Wang and Y. Rojanasakul, *BioMed Res. Int.*, 2013, **2013**, 942916.

